ANTENNA MEASUREMENT REPORT

8000-6230422-230804-01

Characterisation of a

Taoglas PP407096 WLan Antenna

Ordered by

Robert Bosch GmbH
Robert-Bosch-Str. 200
D-31132 Hildesheim
Germany

perfomed at

IMST GmbH
Test Centre Antennas
Carl-Friedrich-Gauss-Str. 2-4
D-47475Kamp-Lintfort
GERMANY

1 TABLE OF CONTENTS

1 Table of Contents 2
2 Figures 3
3 Tables 4
4 General Information 5
5 Preface 6
6 Description and Mounting of the DUTs 7
6.1 DUT Type 7
6.2 Measurement environment 8
6.3 Connection description 8
7 3D-Radiation Pattern and Matching Measurement 9
7.1 Subject 9
7.2 Used measurement devices 9
7.3 Pattern Measurement Setup 10
7.4 Coordinate System During Measurement 11
7.5 Matching measurement 12
7.6 Far field measurement report, results and accuracy 13
8 Far Field Measurement Report 13
9 Results 14
9.1 Max. gain and efficiency 14
9.2 Matching diagrams Taoglas PP407096 antenna port1 15
9.3 Matching diagrams Taoglas PP407096 antenna port2 17
9.4 Pattern diagrams Taoglas PP407096 antenna port1 19
9.5 Pattern diagrams Taoglas PP407096 antenna port2 25
9.6 Intensity diagrams Taoglas PP407096 antenna port1 31
9.7 Intensity diagrams Taoglas PP407096 antenna port2 49

2 FIGURES

Figure 6-1: DUT with connectors. 7
Figure 6-2: DUT Connector marked by IMST. 7
Figure 6-3: Mounting of the DUT. 8
Figure 7-1: Standard setup for pattern measurement. 10
Figure 7-2: Pattern measurement setup. 10
Figure 7-3: Theta/Phi coordinate system. 11
Figure 7-4: Position of the DUT in the theta/phi coordinate system. 11
Figure 7-5: Matching measurement setup. 12
Figure 9-1: Matching diagram, port1 @ 2.4 GHz. 15
Figure 9-2: Matching diagram, port1 @ 5 GHz. 16
Figure 9-3: Matching diagram, port2 @ 2.4 GHz. 17
Figure 9-4: Matching diagram, port2 @ 5 GHz. 18
Figure 9-5: E-Theta/E-Phi/Sum polar diagram, port1 @ 2412 MHz. 19
Figure 9-6: E-Theta/E-Phi/Sum polar diagram, port1 @ 2448 MHz. 20
Figure 9-7: E-Theta/E-Phi/Sum polar diagram, port1 @ 2484 MHz. 21
Figure 9-8: E-Theta/E-Phi/Sum polar diagram, port1 @ 5180 MHz. 22
Figure 9-9: E-Theta/E-Phi/Sum polar diagram, port1 @ 5502.5 MHz. 23
Figure 9-10: E-Theta/E-Phi/Sum polar diagram, port1 @ 5825 MHz. 24
Figure 9-11: E-Theta/E-Phi/Sum polar diagram, port2 @ 2412 MHz. 25
Figure 9-12: E-Theta/E-Phi/Sum polar diagram, port2 @ 2448 MHz. 26
Figure 9-13: E-Theta/E-Phi/Sum polar diagram, port2 @ 2484 MHz. 27
Figure 9-14: E-Theta/E-Phi/Sum polar diagram, port2 @ 5180 MHz. 28
Figure 9-15: E-Theta/E-Phi/Sum polar diagram, port2 @ 5502.5 MHz. 29
Figure 9-16: E-Theta/E-Phi/Sum polar diagram, port2 @ 5825 MHz. 30
Figure 9-17: E-Theta intensity diagram, port1 @ 2412 MHz. 31
Figure 9-18: E-Phi intensity diagram, port1 @ 2412 MHz. 32
Figure 9-19: Sum intensity diagram, port1 @ 2412 MHz. 33
Figure 9-20: E-Theta intensity diagram, port1 @ 2448 MHz. 34
Figure 9-21: E-Phi intensity diagram, port1 @ 2448 MHz. 35
Figure 9-22: Sum intensity diagram, port1 @ 2448 MHz. 36
Figure 9-23: E-Theta intensity diagram, port1 @ 2484 MHz. 37
Figure 9-24: E-Phi intensity diagram, port1 @ 2484 MHz. 38
Figure 9-25: Sum intensity diagram, port1 @ 2484 MHz. 39
Figure 9-26: E-Theta intensity diagram, port1 @ 5180 MHz. 40
Figure 9-27: E-Phi intensity diagram, port1 @ 5180 MHz. 41
Figure 9-28: Sum intensity diagram, port1 @ 5180 MHz. 42
Figure 9-29: E-Theta intensity diagram, port1 @ 5502.5 MHz. 43
Figure 9-30: E-Phi intensity diagram, port1 @ 5502.5 MHz. 44
Figure 9-31: Sum intensity diagram, port1 @ 5502.5 MHz. 45
Figure 9-32: E-Theta intensity diagram, port1 @ 5825 MHz. 46
Figure 9-33: E-Phi intensity diagram port1 @ 5825 MHz. 47
Figure 9-34: Sum intensity diagram, port1 @ 5825 MHz. 48
Figure 9-35: E-Theta intensity diagram, port2 @ 2412 MHz. 49
Figure 9-36: E-Phi intensity diagram, port2 @ 2412 MHz. 50
Figure 9-37: Sum intensity diagram, port2 @ 2412 MHz. 51
Figure 9-38: E-Theta intensity diagram, port2 @ 2448 MHz. 52
Figure 9-39: E-Phi intensity diagram, port2 @ 2448 MHz. 53
Figure 9-40: Sum intensity diagram, port2 @ 2448 MHz. 54
Figure 9-41: E-Theta intensity diagram, port2 @ 2484 MHz. 55
Figure 9-42: E-Phi intensity diagram, port2 @ 2484 MHz. 56
Figure 9-43: Sum intensity diagram, port2 @ 2484 MHz. 57
Figure 9-44: E-Theta intensity diagram, port2 @ 5180 MHz. 58
Figure 9-45: E-Phi intensity diagram, port2 @ 5180 MHz. 59
Figure 9-46: Sum intensity diagram, port2 @ 5180 MHz. 60

Figure 9-47: E-Theta intensity diagram, port2 @ 5502.5 MHz 61
Figure 9-48: E-Phi intensity diagram, port2 @ 5502.5 MHz 62
Figure 9-49: Sum intensity diagram, port2 @ 5502.5 MHz 63
Figure 9-50: E-Theta intensity diagram, port2 @ 5825 MHz 64
Figure 9-51: E-Phi intensity diagram port2 @ 5825 MHz 65
Figure 9-52: Sum intensity diagram, port2 @ 5825 MHz 66

3 TABLES

Table 7-1: Devices used for calibration and measurement 9
Table 8-1: Far field measurement report 13
Table 9-1: S11, efficiency and maximum gain of the dual band wlan antenna port1 @ 2.4 GHz. 14
Table 9-2: S11, efficiency and maximum gain of the dual band wlan antenna port1 @ 5 GHz. 14
Table 9-3: S11, efficiency and maximum gain of the dual band wlan antenna port2 @ 2.4 GHz. 14
Table 9-4: S11, efficiency and maximum gain of the dual band wlan antenna port2 @ 5 GHz. 14

4 General Information

Customer : Robert Bosch Car Multi Media GmbH
Mr. Bernd Meyer
Robert-Bosch-Str. 200
D-31132 Hildesheim
Germany

Devices under test (DUT): Taoglas PP407096 two port dual band WLan antenna

Subject: Determination of the Gain, the 3D antenna pattern, the efficiency and the matching at WLan frequencies.

Date of measurement: 26. – 27.04.2023

Performed: Stefan Weitz

Quotation-No.: 5230144-B

Order-No.: 4503542816

Project-No.: 8000_6230422

Department: Antennas & EM Modelling

Responsible: Aline Friedrich
+49-2842-981-337

Performed:..... Reviewed:.....

Stefan Weitz
Test engineer

Aline Friedrich
Head of laboratory

5 PREFACE

In this measurement campaign a two port dual band WLan antennas was measured on a metal plate as described in the following.

The patterns of the DUTs (**D**evices **U**nder **T**est) have been measured three-dimensional at WLan frequencies. The measurements have been done with two orthogonal polarisations of the measurement antenna. After the measurement the efficiencies of the DUT has been determined.

The results are documented as tables and diagrams in chapter 9.

6 Description and Mounting of the DUTs

6.1 DUT Type

The DUT consisted of a plastic case with a two port dual band (2.4 GHz and 5 GHz) WLan antenna and inseparably mounted RF-cables with FAKRA connectors. See Figure 6-1.

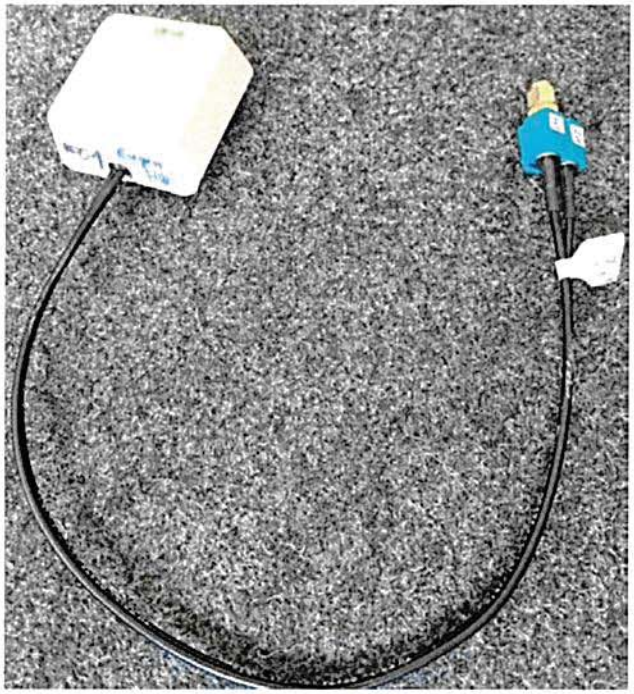

Figure 6-1: DUT with connectors.

The antennas connectors are marked by the IMST as port1 (P1) and port2 (P2) See Figure 6-2.

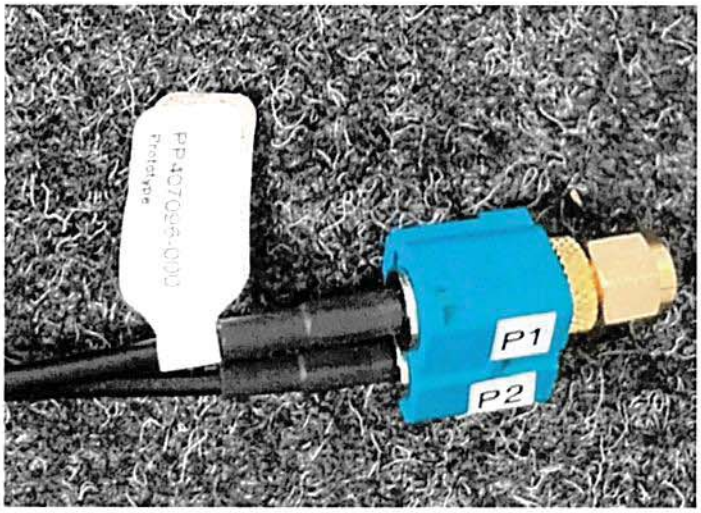

Figure 6-2: DUT Connector marked by IMST.

Because of the inseparably mounted RF-cable antenna and cable has been treated as one unit.

6.2 Measurement environment

The measurements have been performed in the air conditioned and completely shielded anechoic chamber (Range II) B83117-A1431-T161 of IMST GmbH. This minimizes measurement errors caused by variations in temperature, disturbing signals and reflections.

Movement of the DUT has been done by a „Roll over Azimuth"-positioner. The Mast that carries the roll axis is made from Kevlar™. The accuracy of the azimuth positioner is 0.03°. During measurement the azimuth positioner is covered with absorbers.

The following figure shows the mounting of the DUT for the measurement.

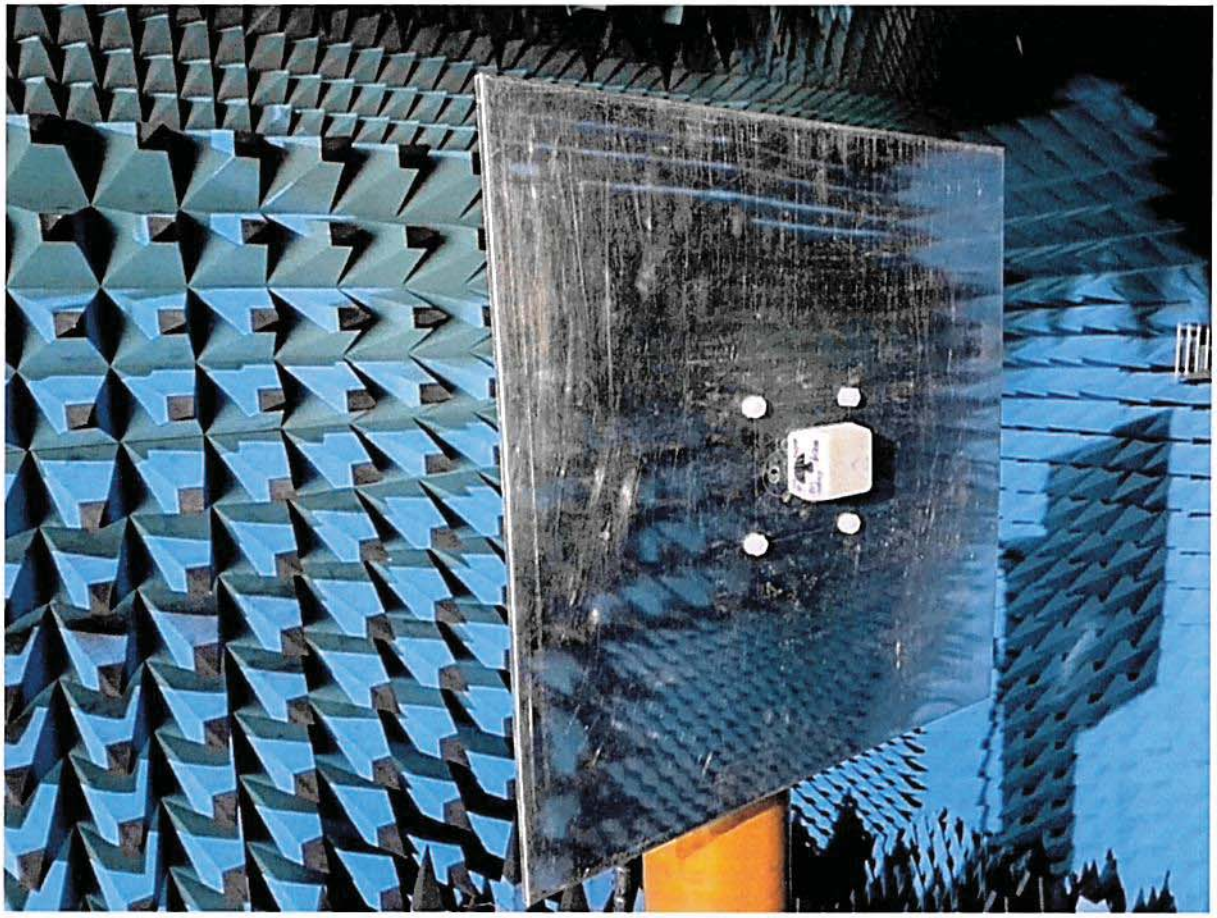

Figure 6-3: Mounting of the DUT.

During measurement the DUT was mounted on a metal sheet (50 x 50 cm) provided by IMST.

The distance between the measurement antenna and the rotation centre of the DUT was ca. 2.23 m during measurement (Far field conditions).

6.3 Connection description

To minimize errors caused by mismatching the feeding cable was equipped with an attenuator with a very low VSWR. The SMA connector of the attenuator was the reference plane for the pattern measurement. FAKRA-to-SMA-Adapters were provided by IMST.

All unused ports of the DUT were terminated by a 50 ohm load during measurement.

During measurement no actions were taken to suppress surface waves.

7 3D-Radiation Pattern and Matching Measurement

7.1 Subject

The three-dimensional antenna pattern measurements with two orthogonal polarisations of the measurement antenna enable the determination of the gain and the efficiency.

The matching measurement shows the S_{11} of the DUT over measured frequency range.

7.2 Used measurement devices

All calibrations and measurements have been done with the devices that are stated in the following table. The date of the last calibration is shown in the column "Cal. Date".

Type	Device	Ser. No.	Cal. Date
ZVL Rohde & Schwarz	Network/Spectrum analyser 9 kHz – 13.6 GHz	10114	07.2019
SH800 Satimo	Dual ridged Horn (Ref. Ant.) 0.8 -12.0GHz	79	08.2019
SH800 Satimo	Dual ridged Horn (Meas. Ant.) 0.8 -12.0GHz	78	08.2019
SH800 Satimo	Dual ridged Horn (Meas. Ant.) 0.8 -12.0GHz	77	08.2019
B83117-A1431-T161 Siemens Matsushita	Anechoic Chamber	Project No. 007-A34-089/99A	N/A
AL-DBDR-3G/AL-560 Orbit/FR	Roll-over-azimuth positioner	434	N/A
AL-4164-MC Orbit/FR	Controller	25	N/A
DARIC 2.0 IMST	Control and measurement software		N/A
Rohacell bracket	Free space mounting		N/A
S8150 Copper Mountain	2 Port Vector Network analyzer 100 kHz - 18 GHz	21280020	08.2021
02CK10A-150 Rosenberger	Calibration Kit DC – 40 GHz	U3901	07.2019

Table 7-1: Devices used for calibration and measurement

7.3 Pattern Measurement Setup

Figure 7-1 shows the principle setup for the pattern measurement.

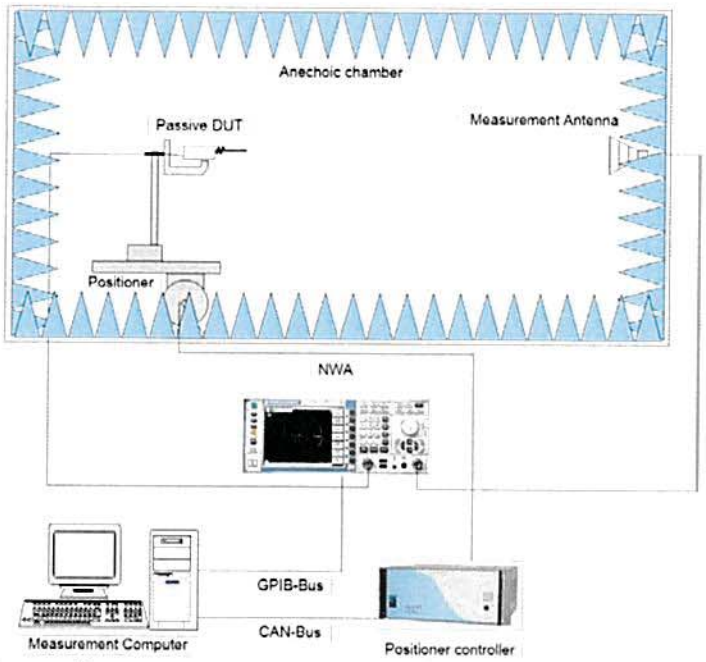

Figure 7-1: Standard setup for pattern measurement.

Figure 7-2 shows the mechanical pattern measurement setup. It is a standard setup for small antenna measurement. Additional setup information could be found in chapter 6.2.

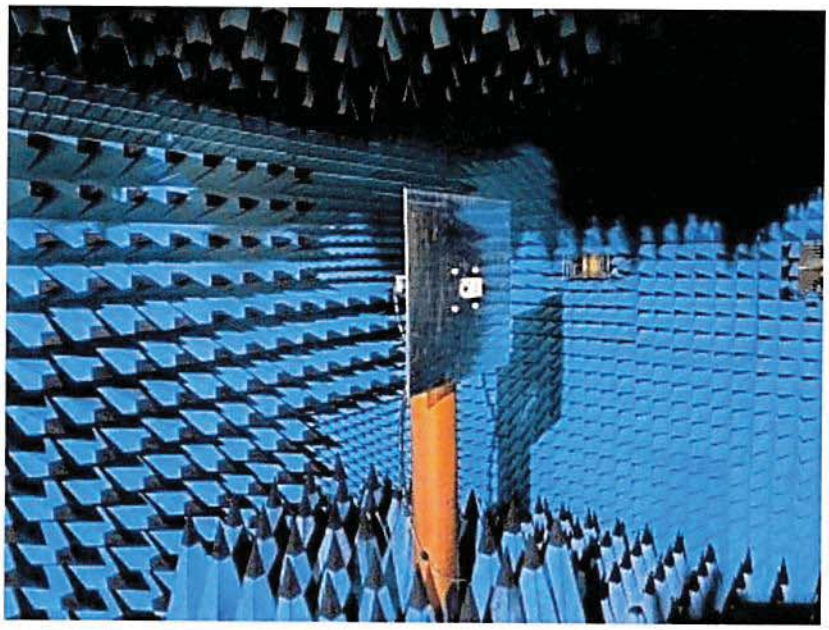

Figure 7-2: Pattern measurement setup.

For calibration and pattern measurement broad band horns type SH800 from Satimo (Microwave Vision Company, MVC) has been used.

Before the calibration was done the position of the measurement and the calibration antenna was checked by a positioning laser. The same procedure was used for the positioning of the DUT.

7.4 Coordinate System During Measurement

For the measurements the theta/phi coordinate system has been used as shown in Figure 7-3. Also the movement of the measurement antenna (MA) with its polarisations are shown.

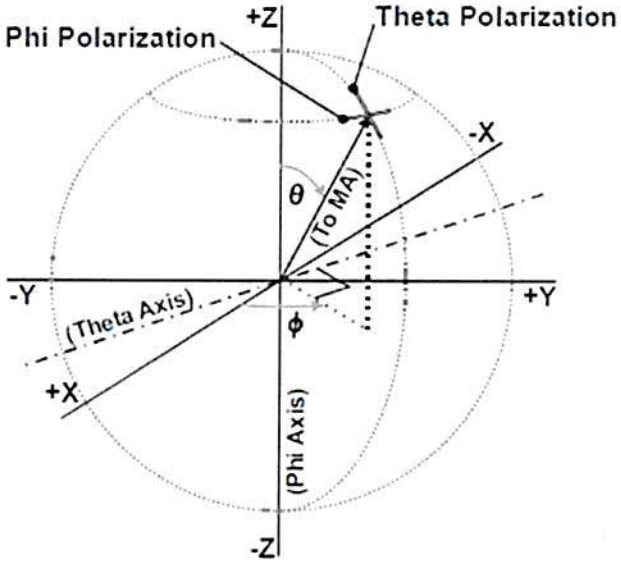

Figure 7-3: Theta/Phi coordinate system.

In Figure 7-4 the position of the DUT in the theta/phi coordinate system is shown which has been used for measurement and evaluation.

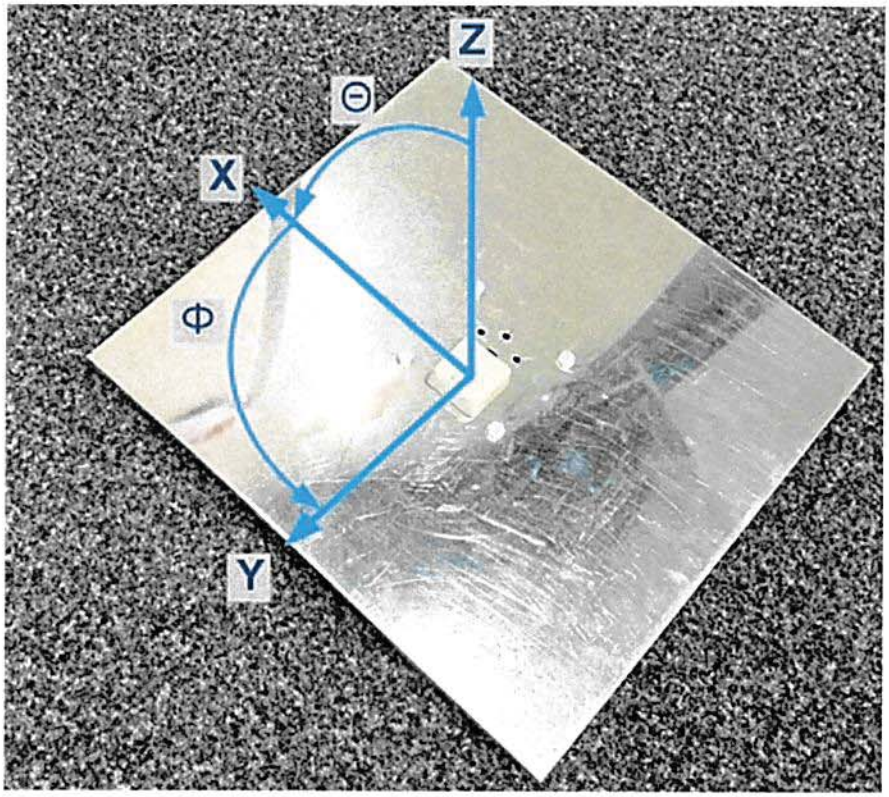

Figure 7-4: Position of the DUT in the theta/phi coordinate system

7.5 Matching measurement

The following picture shows the setup of the matching (S_{11}/S_{22}) measurement.

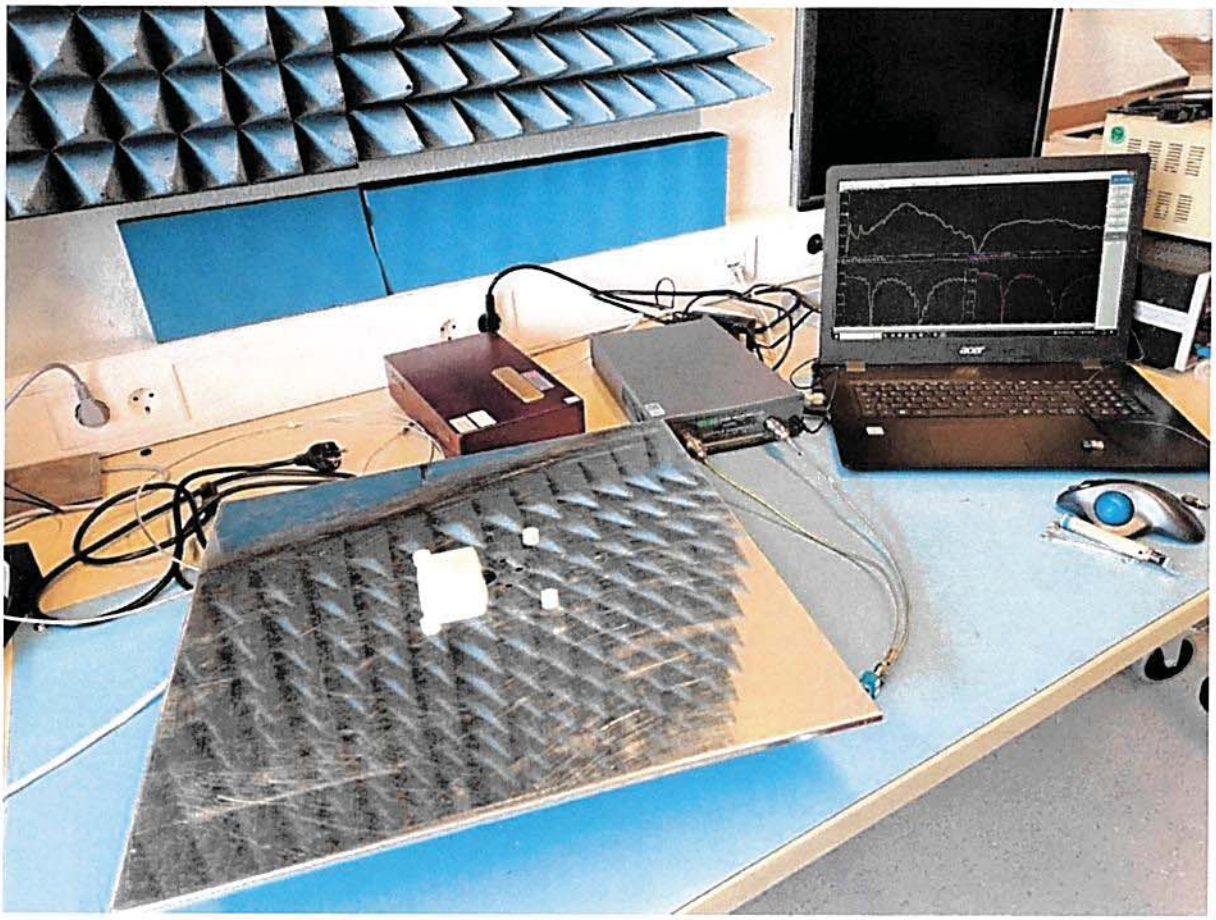

Figure 7-5: Matching measurement setup.

During matching measurement the DUT was located on a Styrofoam block. This minimizes external influence of the measurement results. The matching measurement was performed over a frequency range from 1000 MHz up to 7000 MHz with a resolution of 24001 points. The 2-port NWA S5810 from Copper Mountain was calibrated with a full-two-port calibration. The calibration was performed with the 02CK10-ARPC-2.92 calibration kit from Rosenberger.

7.6 Far field measurement report, results and accuracy

The "Far field measurement report" in chapter 8 gives an overview about the performed measurements.

The results of the 3d antenna pattern measurement, the efficiency evaluation and the matching measurement are shown in chapter 9.

The accuracy of the measurement results has been specified with ±1 dB.

8 Far Field Measurement Report

FF-Measurement-Report

Operator: SW
Date from: 26.- 27.04.2023
Project: 8000_6230422
Object: 2-Port dual band WLan antenna
Temp: 23°C +/-1°

Setup-Files	Frequencies / MHz	
S1: n/a	f1: 1000 - 7000	24001 points
S2: Bosch_CMM.dam	f2: 2412 - 2484	3 points
	f3: 5180 - 5825	3 points

No.	File	Frequency /MHz	Meas.-Axis	Step-Axis		Remarks	Setupfile
			Roll/°	Azimuthl/°	Polarisation		
1	PP407096_S-Par.s2p	f1	n/a	n/a	n/a		
2	20230426_085125_Taoglas_PP407096_Dual_band_WLan_P1	f2, f3	0/+355 (5)	0/+180 (5)	Theta/Phi		S2
3	20230426_102118_Taoglas_PP407096_Dual_band_WLan_P2	"	"	"	"		"

Table 8-1: Far field measurement report

9 RESULTS

9.1 Max. gain and efficiency

The following table shows the matching and efficiency values of the DUT. Also measurement angles with maximum gain values are shown.

	f	S11	η	Max. Gain at Polarisation Θ			Max. Gain at Polarisation Φ			Max. Gain absolut		
Taoglas PP407096 Dual Band Wlan Antenna, P1 @ 2.4 GHz	MHz	dB	%	dBi	Θ [°]	Φ [°]	dBi	Θ [°]	Φ [°]	dBi	Θ [°]	Φ [°]
	2412	-16.63	55.5	4.2	65	310	-2.9	30	275	4.4	65	305
	2448	-10.42	51.1	4.1	62	305	-3.2	30	275	4.3	65	305
	2484	-8.67	47.1	3.7	65	305	-3.4	35	275	3.9	62	305

Table 9-1: S11, efficiency and maximum gain of the dual band wlan antenna port1 @ 2.4 GHz.

	f	S11	η	Max. Gain at Polarisation Θ			Max. Gain at Polarisation Φ			Max. Gain absolut		
Taoglas PP407096 Dual Band Wlan Antenna, P1 @ 5 GHz	MHz	dB	%	dBi	Θ [°]	Φ [°]	dBi	Θ [°]	Φ [°]	dBi	Θ [°]	Φ [°]
	5180	-17.23	18.0	0.8	70	360	-2.9	35	255	0.8	70	360
	5502.5	-7.45	17.2	0.3	70	340	-1.4	40	225	0.3	70	340
	5825	-5.83	16.7	0.9	70	350	-2.6	40	230	0.9	70	350

Table 9-2: S11, efficiency and maximum gain of the dual band wlan antenna port1 @ 5 GHz.

	f	S11	η	Max. Gain at Polarisation Θ			Max. Gain at Polarisation Φ			Max. Gain absolut		
Taoglas PP407096 Dual Band Wlan Antenna, P2 @ 2.4 GHz	MHz	dB	%	dBi	Θ [°]	Φ [°]	dBi	Θ [°]	Φ [°]	dBi	Θ [°]	Φ [°]
	2412	-30.34	58.6	4.8	65	70	-2.5	30	85	5.0	65	70
	2448	-14.80	57.8	4.9	65	60	-2.6	30	85	5.1	65	55
	2484	-11.22	54.9	4.7	65	55	-2.7	35	85	4.9	65	55

Table 9-3: S11, efficiency and maximum gain of the dual band wlan antenna port2 @ 2.4 GHz.

	f	S11	η	Max. Gain at Polarisation Θ			Max. Gain at Polarisation Φ			Max. Gain absolut		
Taoglas PP407096 Dual Band Wlan Antenna, P2 @ 5 GHz	MHz	dB	%	dBi	Θ [°]	Φ [°]	dBi	Θ [°]	Φ [°]	dBi	Θ [°]	Φ [°]
	5180	-26.78	17.2	0.6	70	355	-2.6	25	95	0.7	70	355
	5502.5	-9.37	17.1	-0.2	75	25	-1.5	50	120	0.3	70	105
	5825	-6.34	18.7	0.8	70	355	-1.2	40	130	0.9	70	105

Table 9-4: S11, efficiency and maximum gain of the dual band wlan antenna port2 @ 5 GHz.

9.2 Matching diagrams Taoglas PP407096 antenna port1

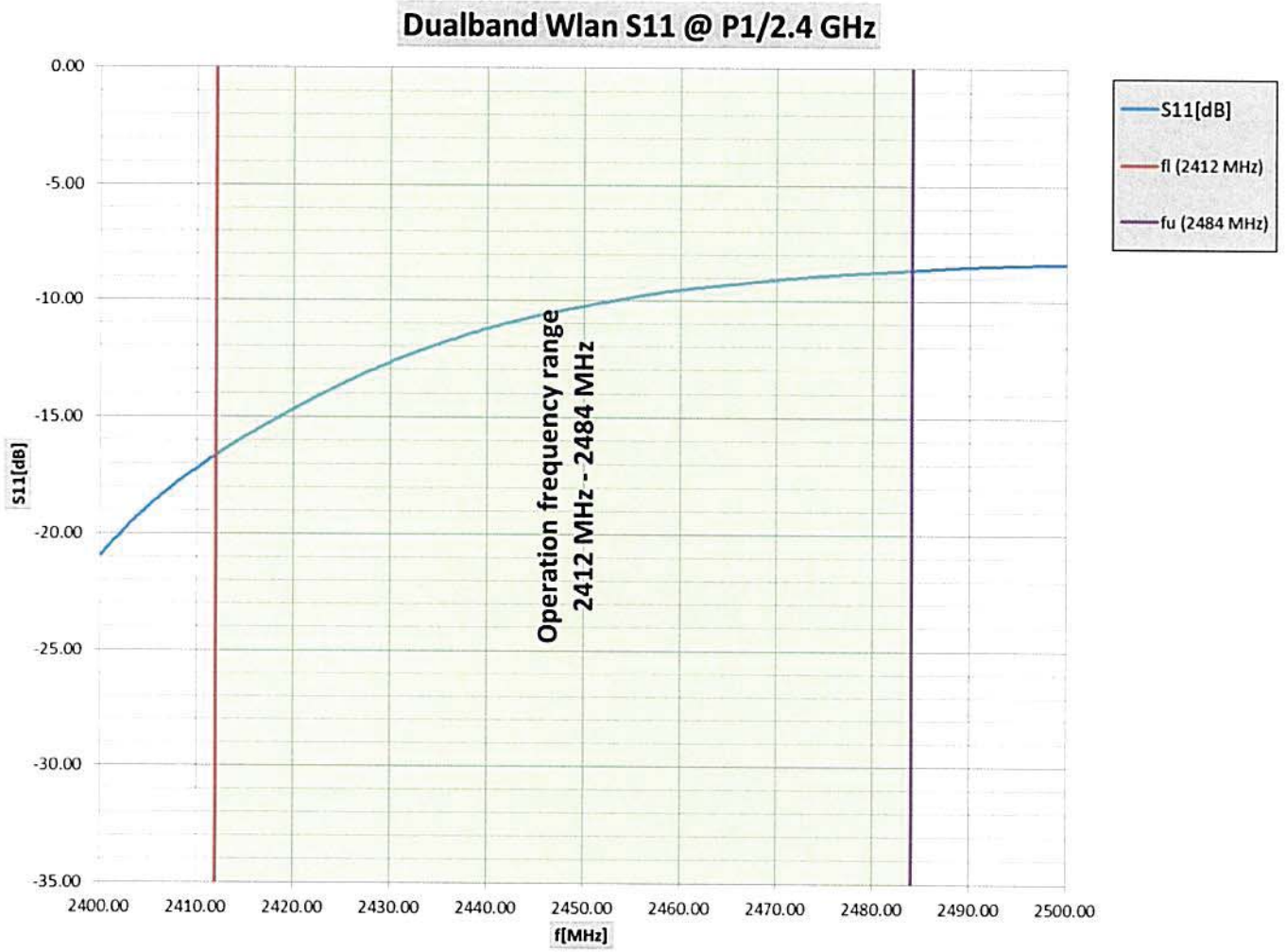

Figure 9-1: Matching diagram, port1 @ 2.4 GHz

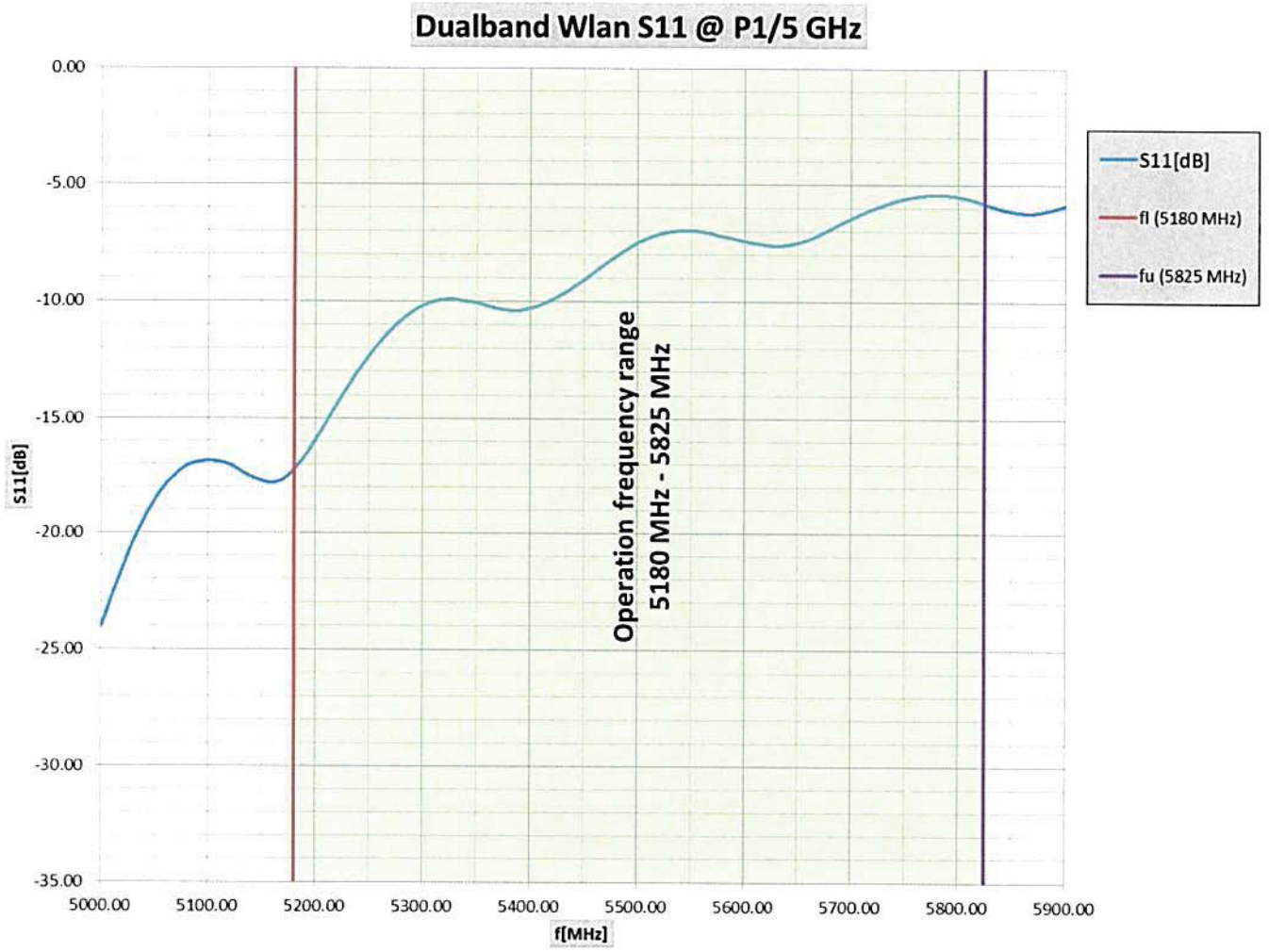

Figure 9-2: Matching diagram, port1 @ 5 GHz

9.3 Matching diagrams Taoglas PP407096 antenna port2

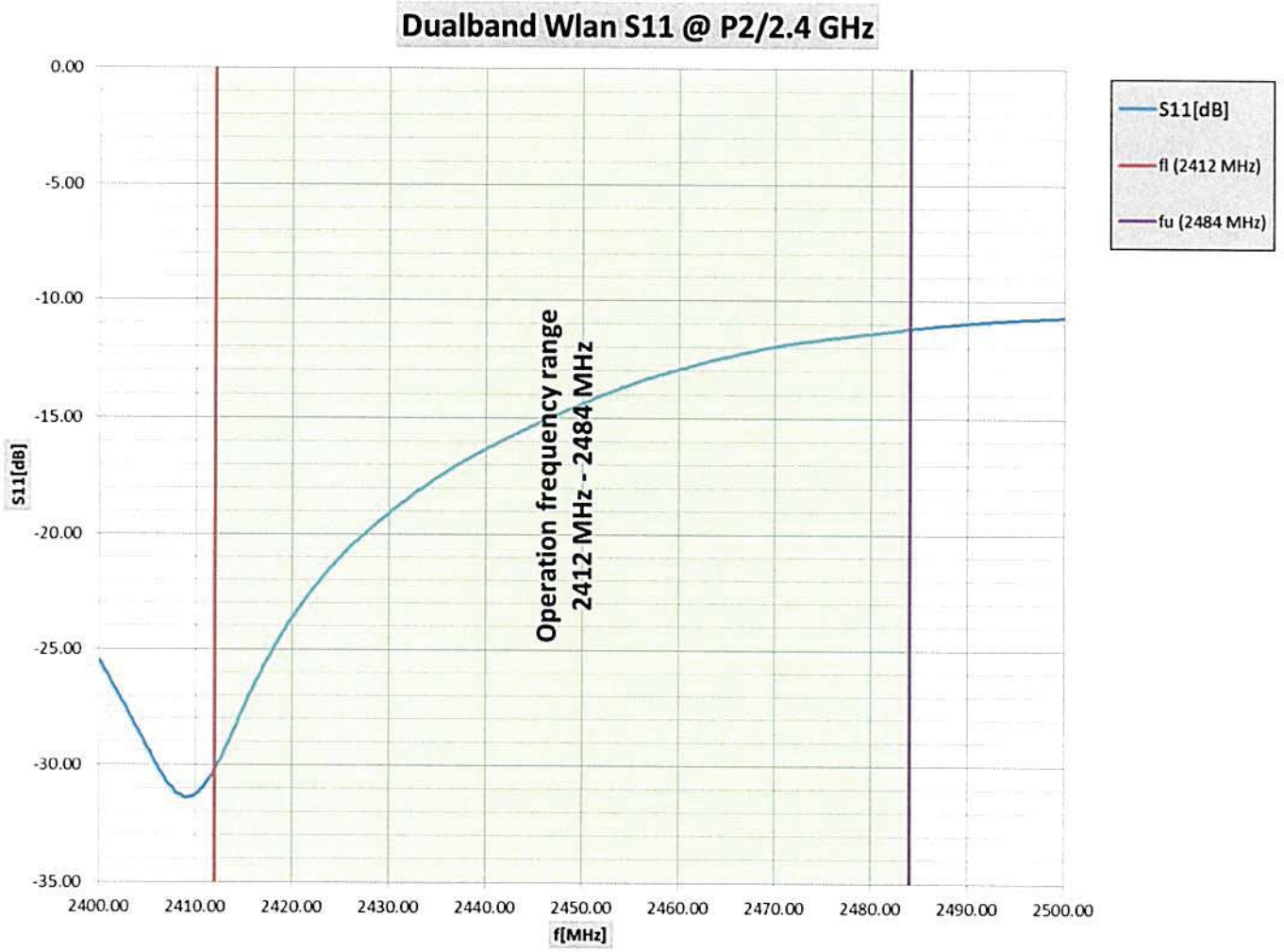

Figure 9-3: Matching diagram, port2 @ 2.4 GHz

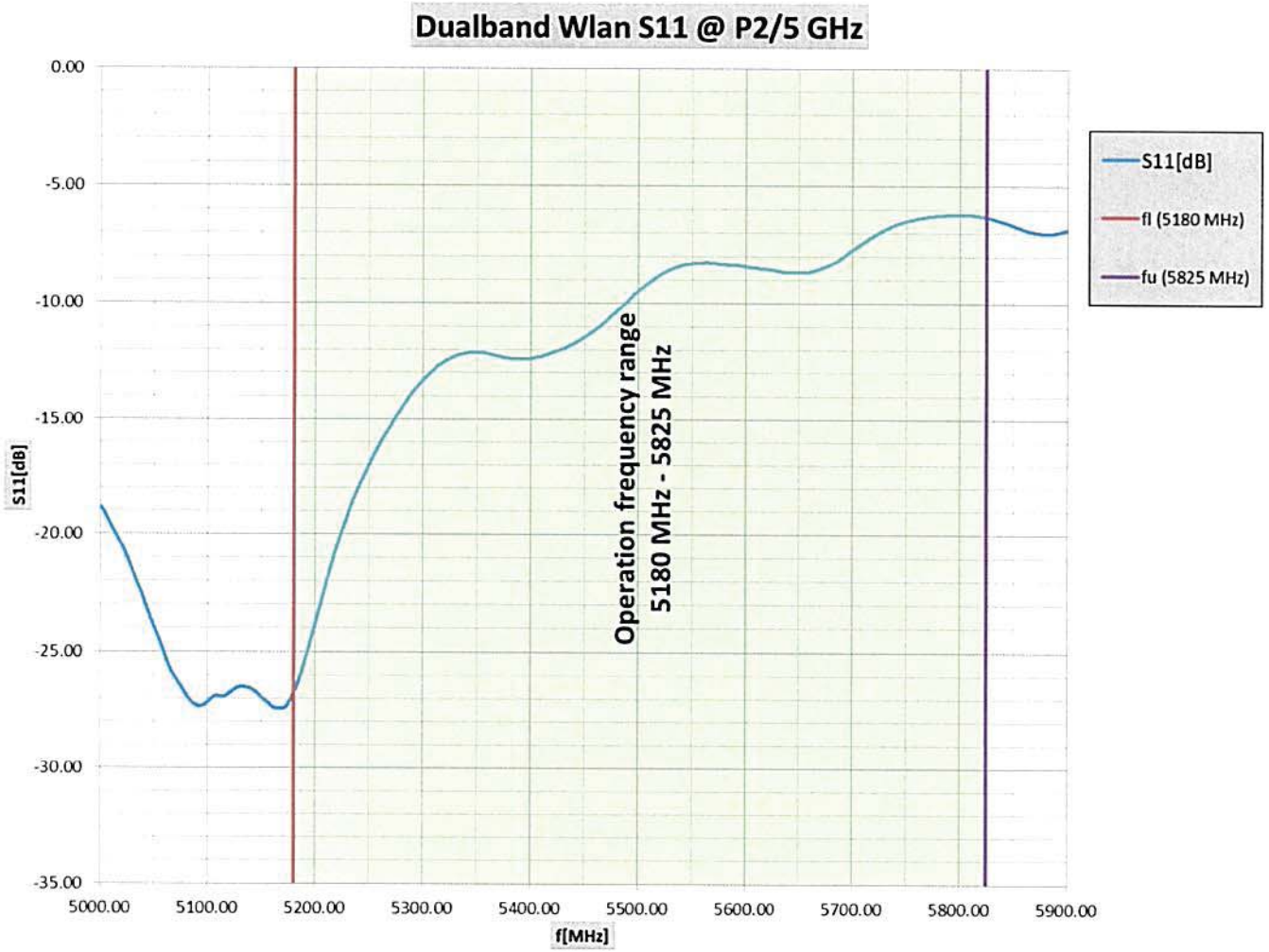

Figure 9-4: Matching diagram, port2 @ 5 GHz

9.4 Pattern diagrams Taoglas PP407096 antenna port1

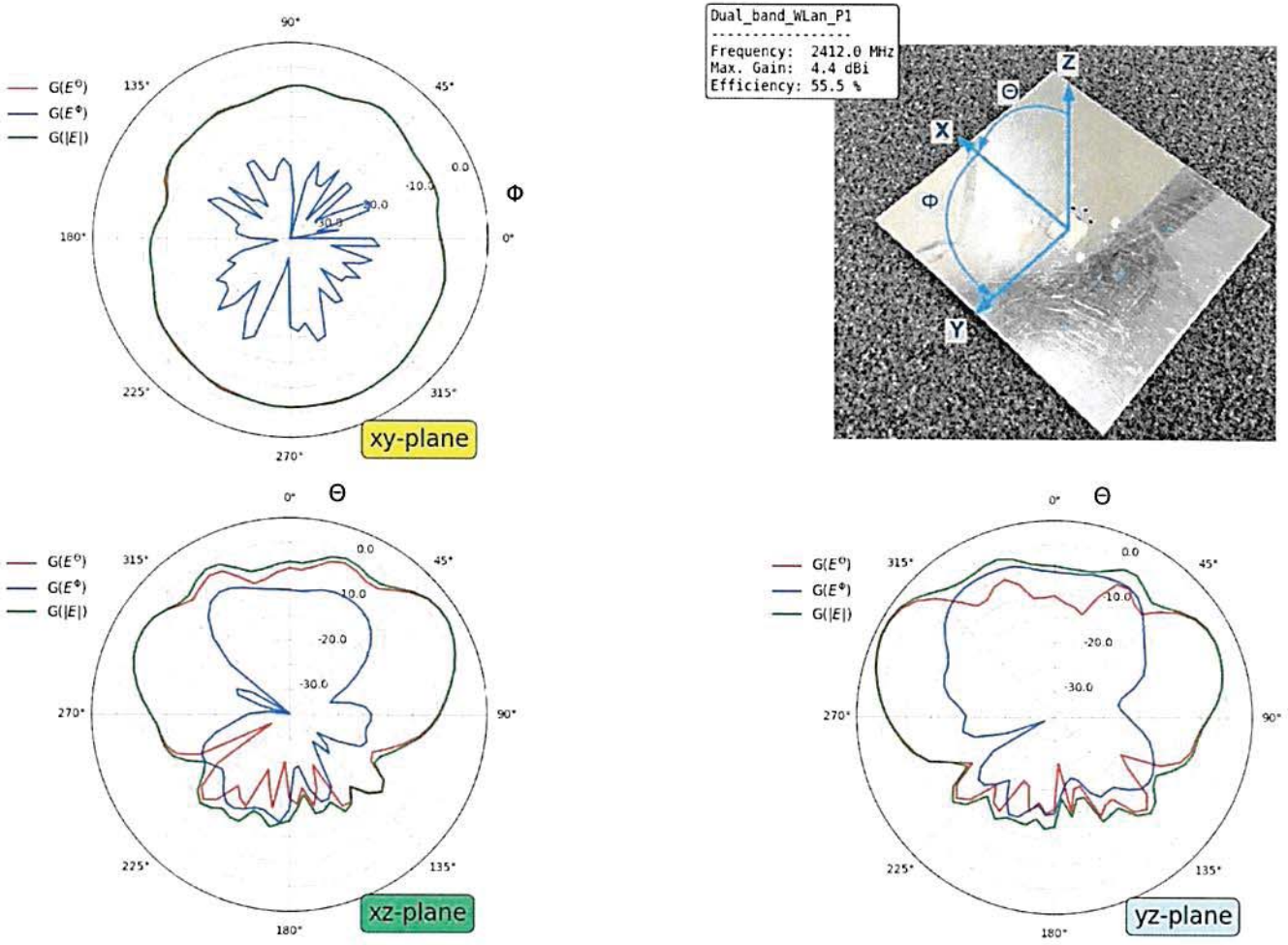

Figure 9-5: E-Theta/E-Phi/Sum polar diagram, port1 @ 2412 MHz

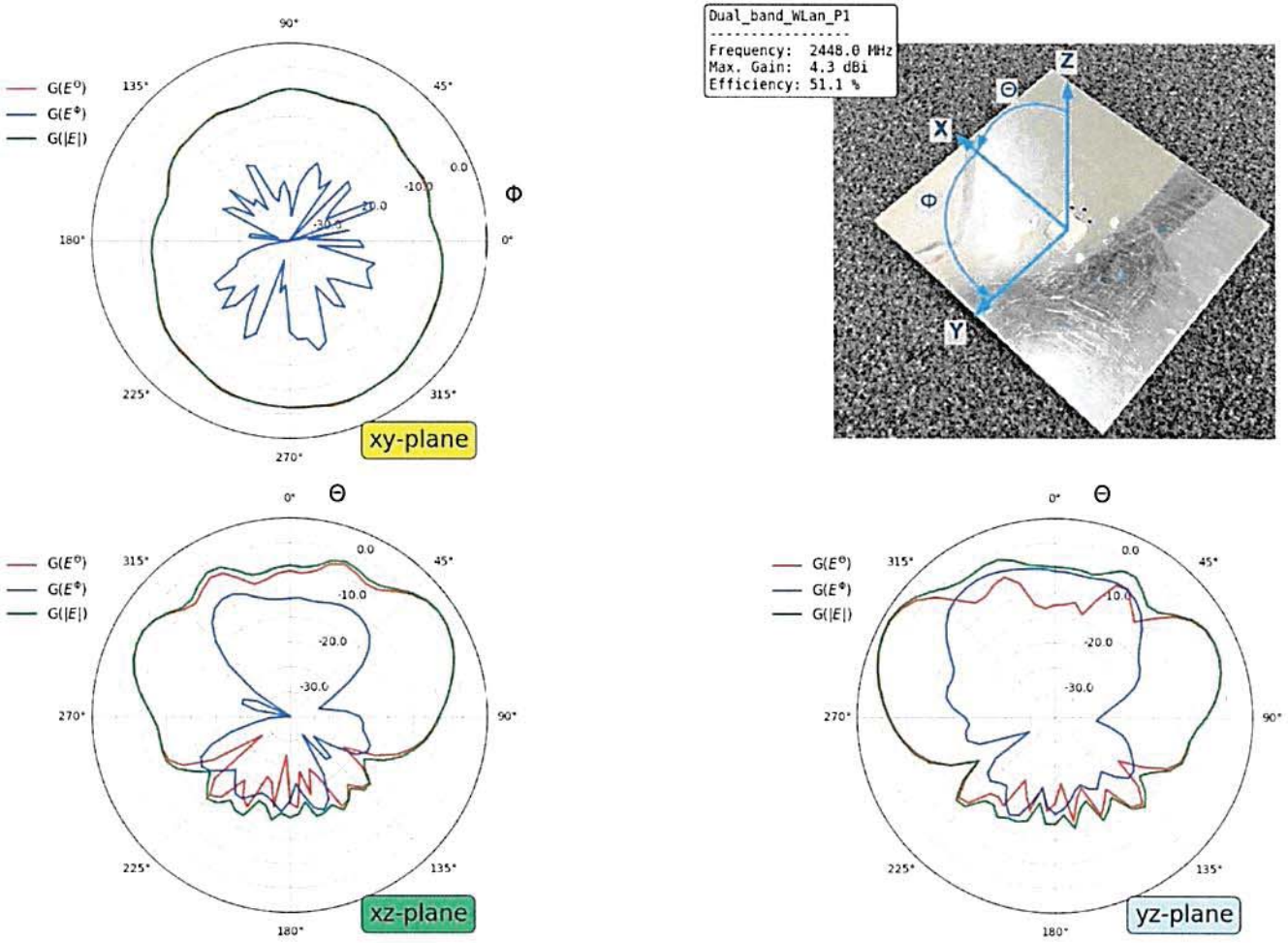

Figure 9-6: E-Theta/E-Phi/Sum polar diagram, port1 @ 2448 MHz

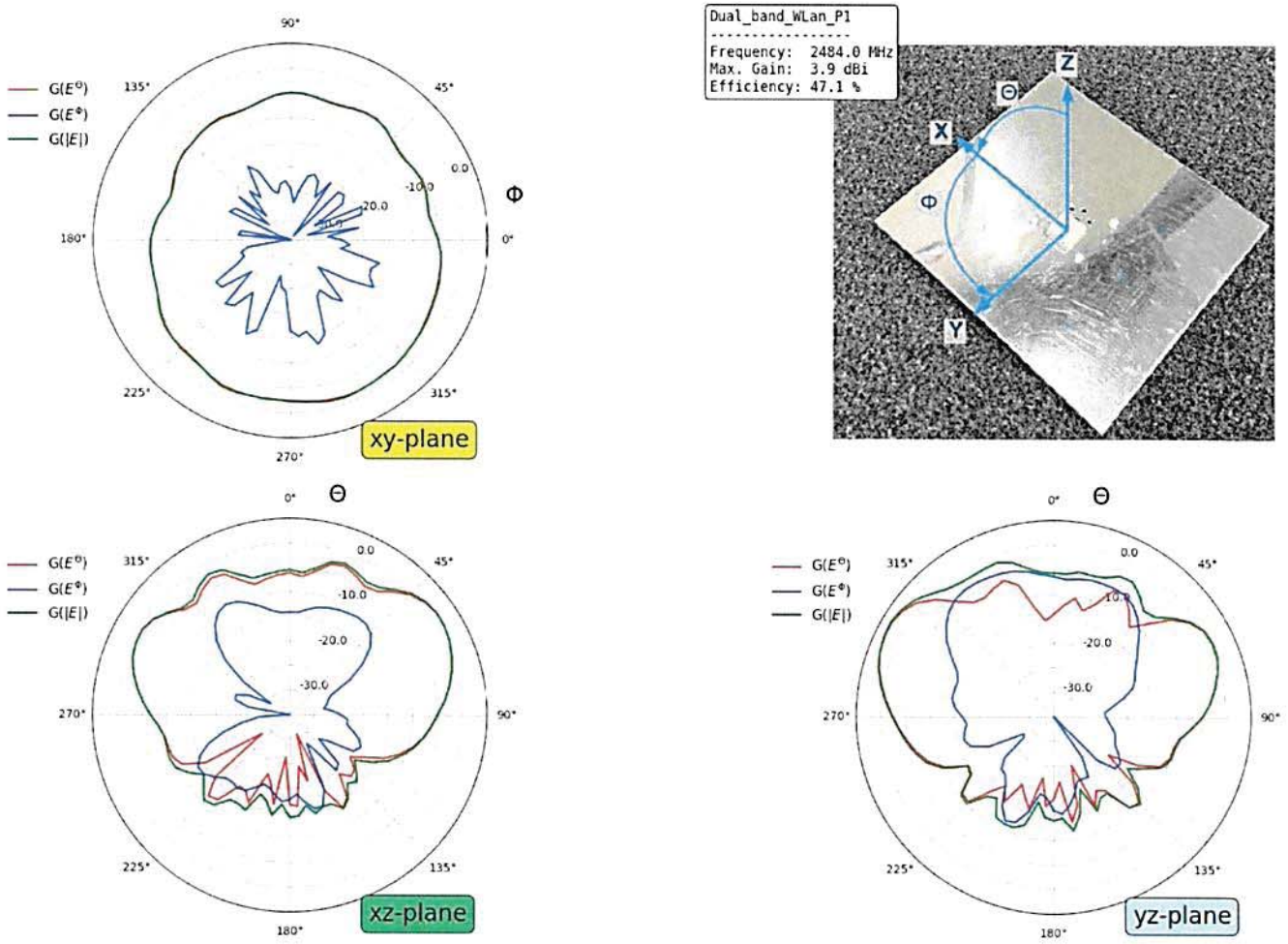

Figure 9-7: E-Theta/E-Phi/Sum polar diagram, port1 @ 2484 MHz

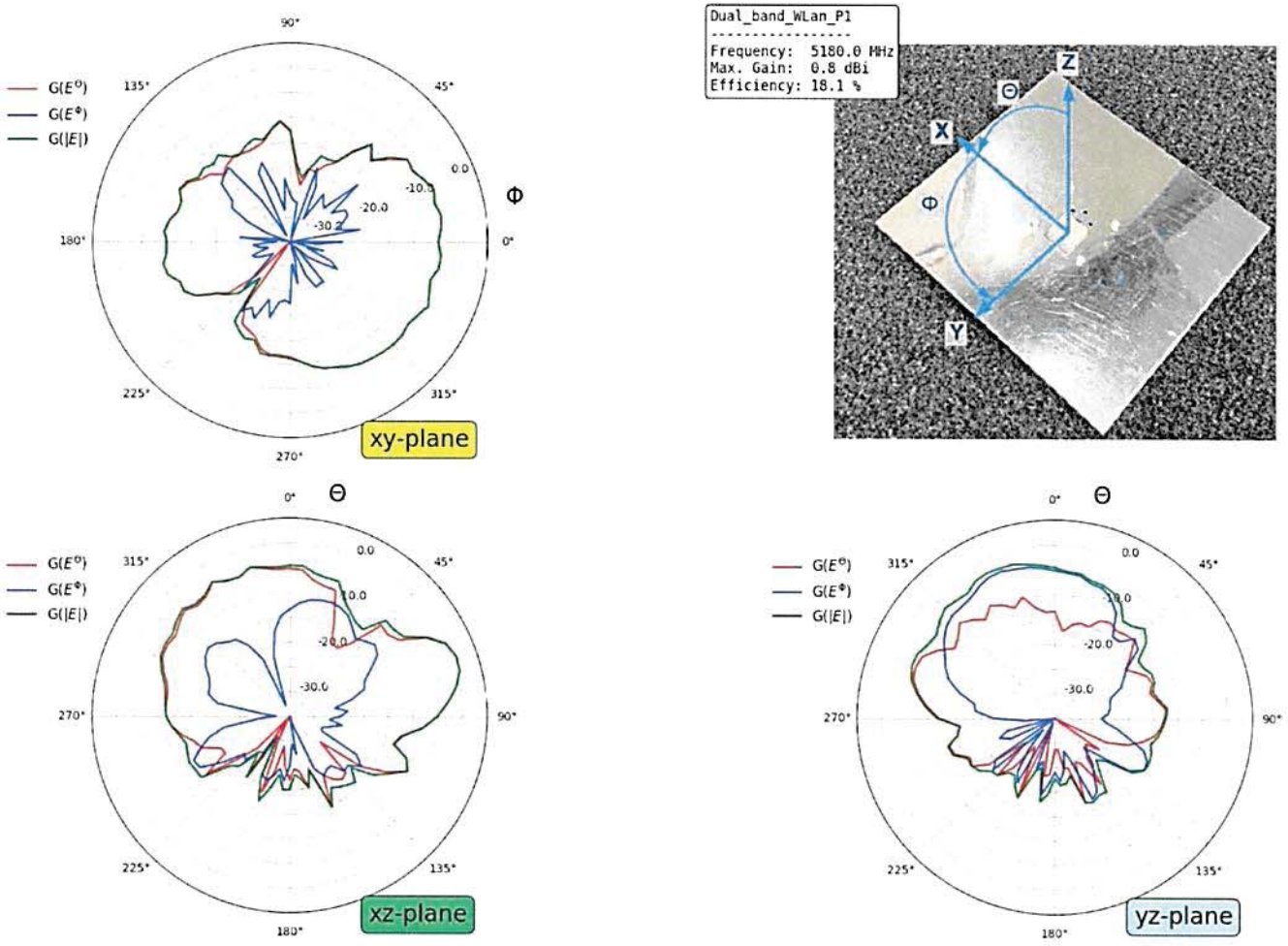

Figure 9-8: E-Theta/E-Phi/Sum polar diagram, port1 @ 5180 MHz

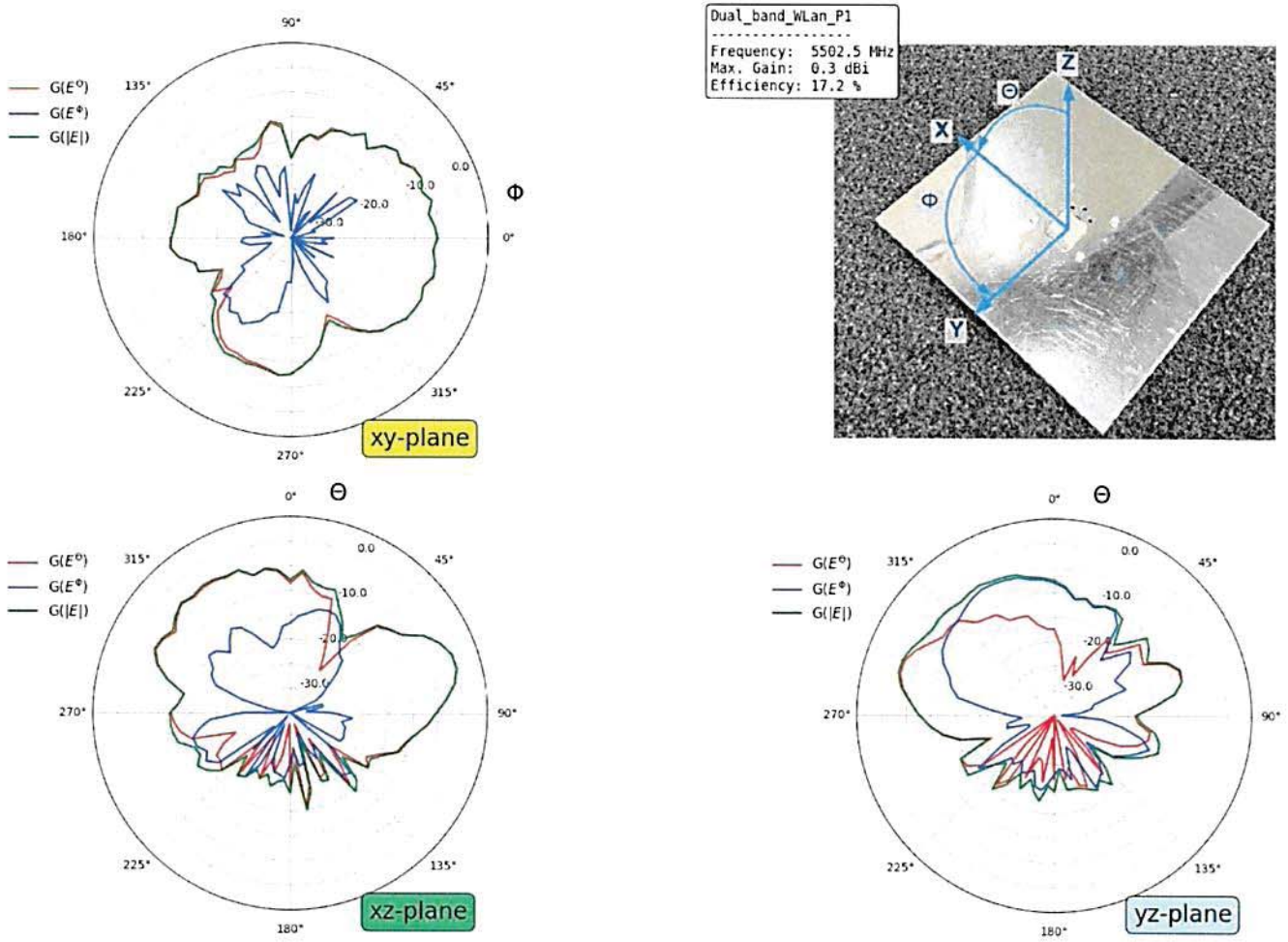

Figure 9-9: E-Theta/E-Phi/Sum polar diagram, port1 @ 5502.5 MHz

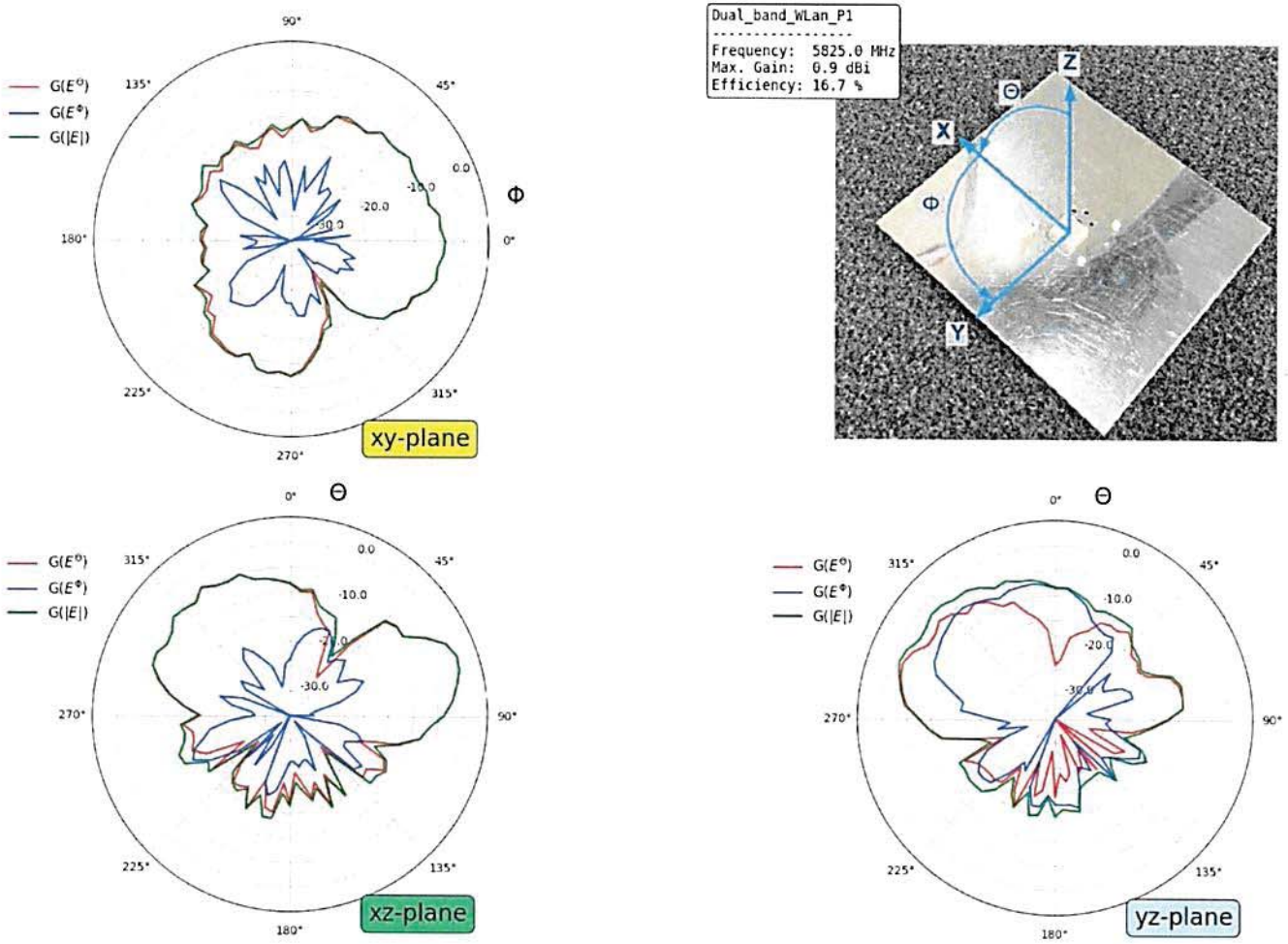

Figure 9-10: E-Theta/E-Phi/Sum polar diagram, port1 @ 5825 MHz

9.5 Pattern diagrams Taoglas PP407096 antenna port2

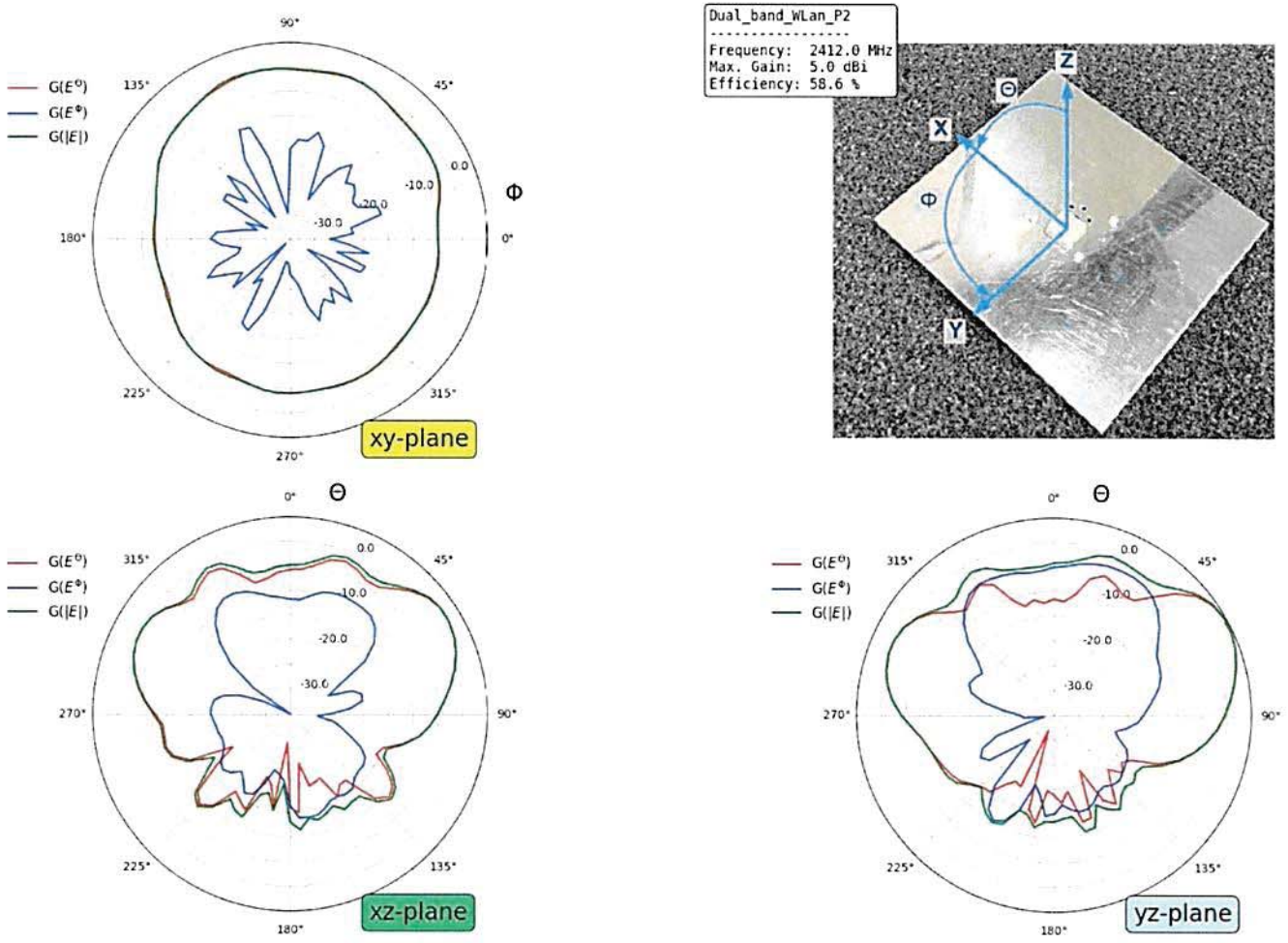

Figure 9-11: E-Theta/E-Phi/Sum polar diagram, port2 @ 2412 MHz

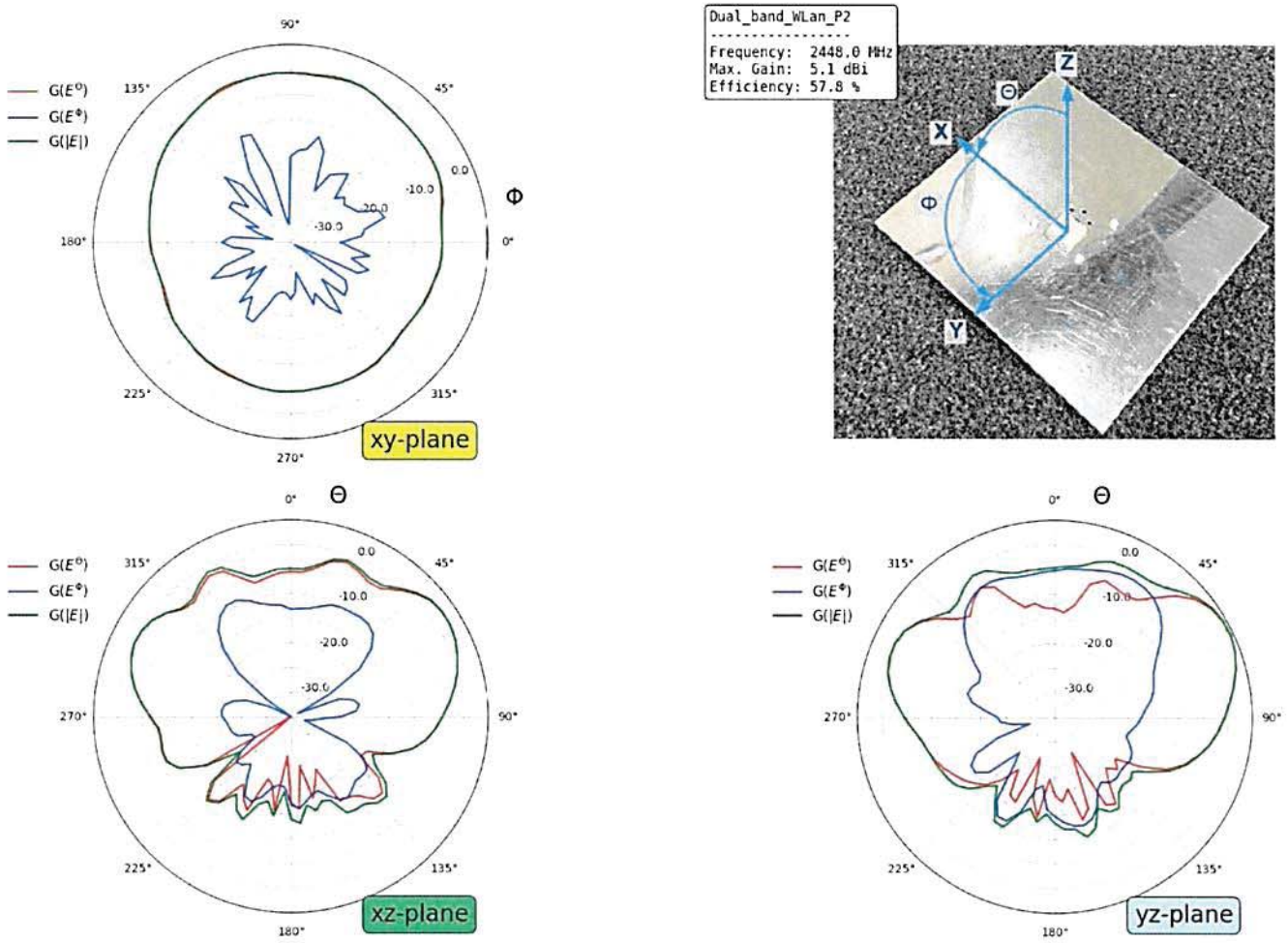

Figure 9-12: E-Theta/E-Phi/Sum polar diagram, port2 @ 2448 MHz

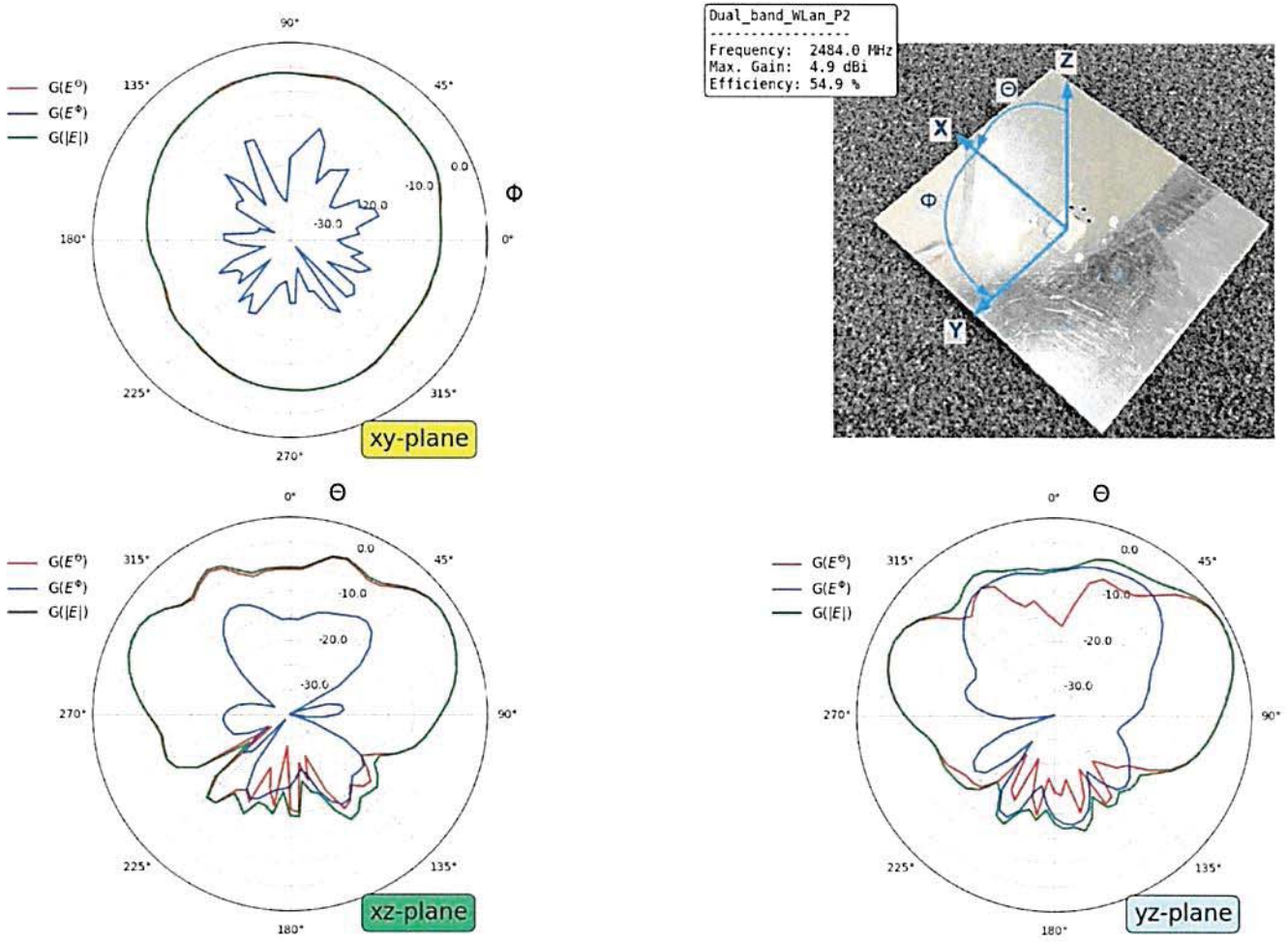

Figure 9-13: E-Theta/E-Phi/Sum polar diagram, port2 @ 2484 MHz

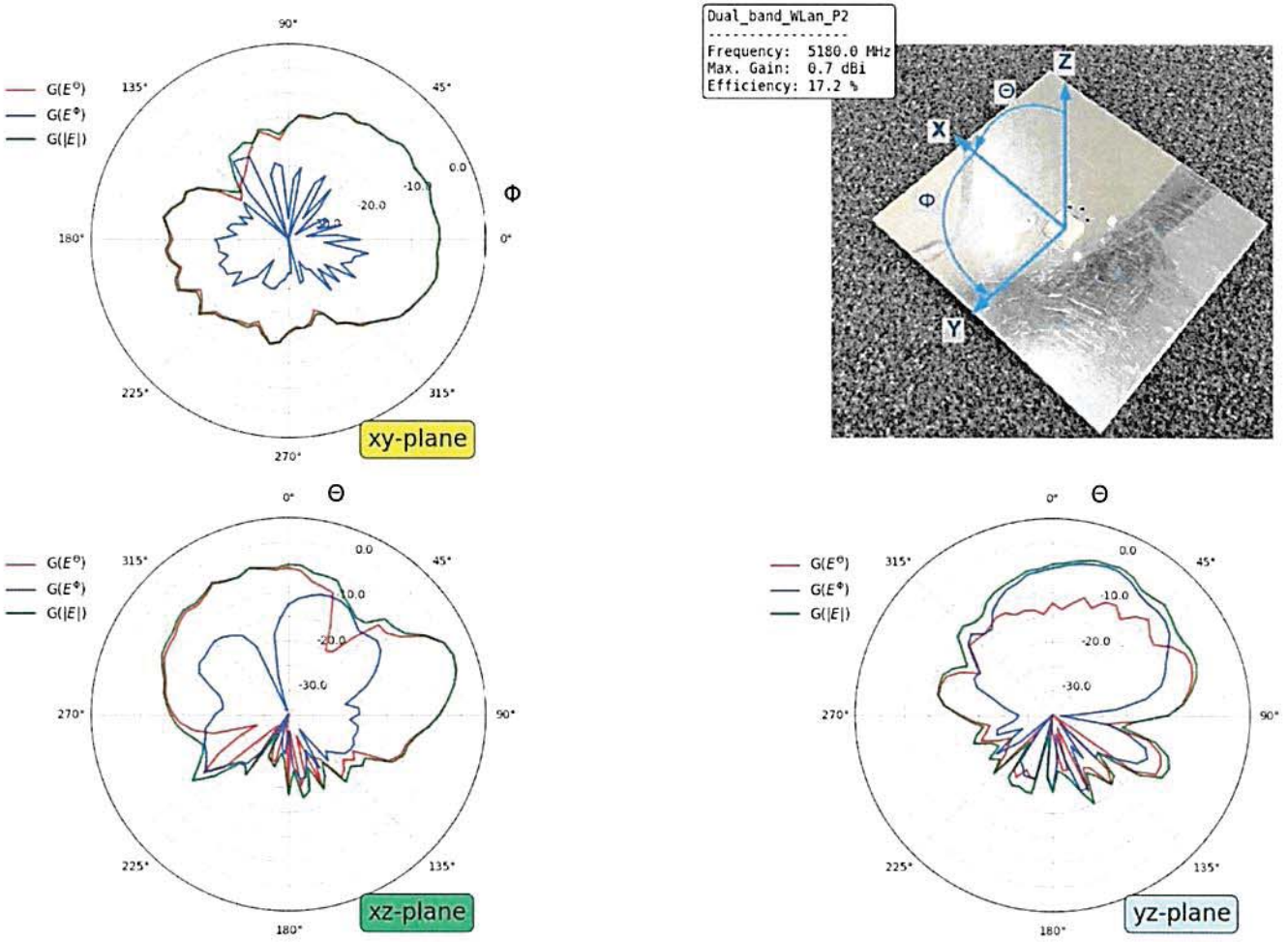

Figure 9-14: E-Theta/E-Phi/Sum polar diagram, port2 @ 5180 MHz

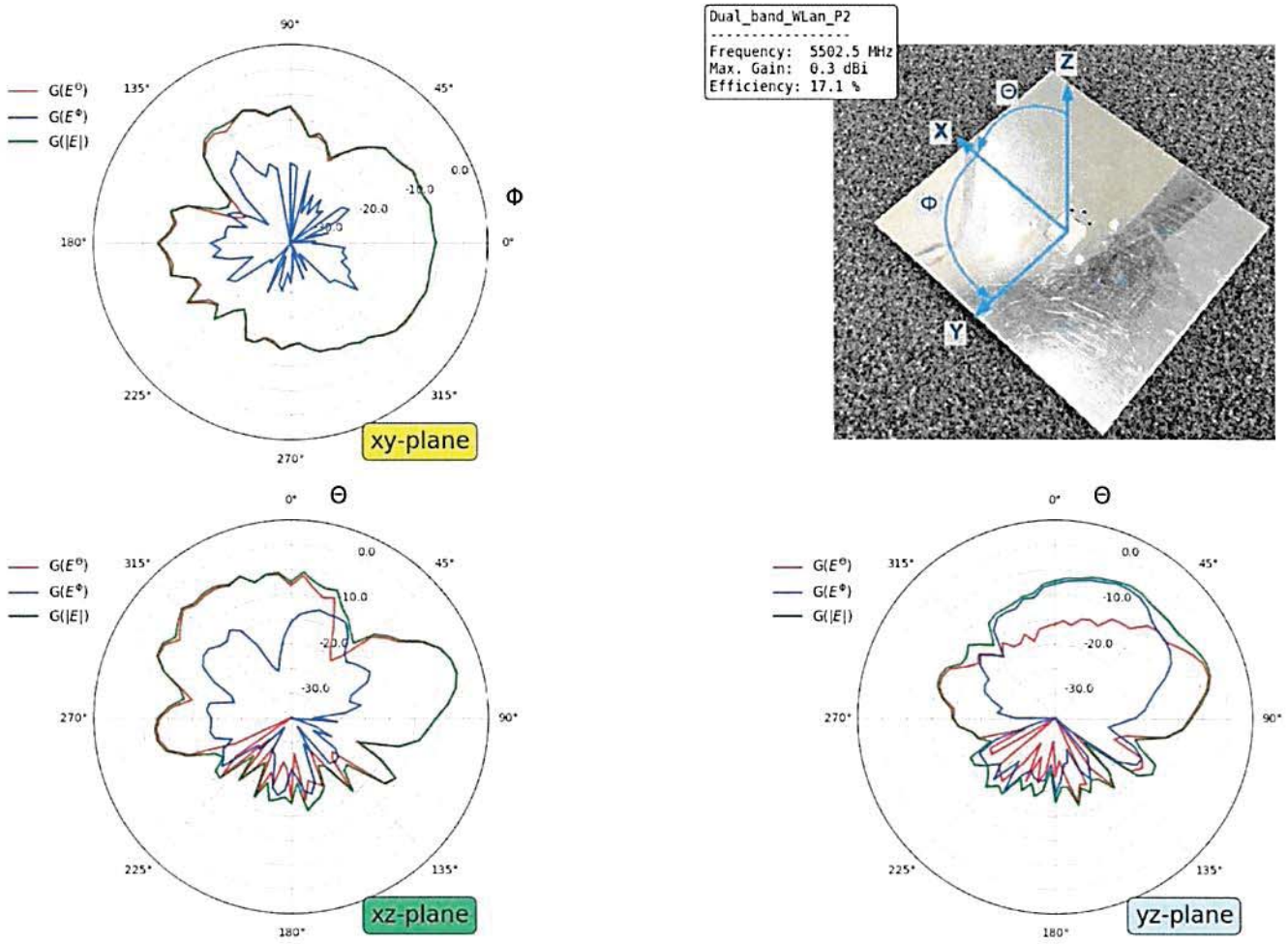

Figure 9-15: E-Theta/E-Phi/Sum polar diagram, port2 @ 5502.5 MHz

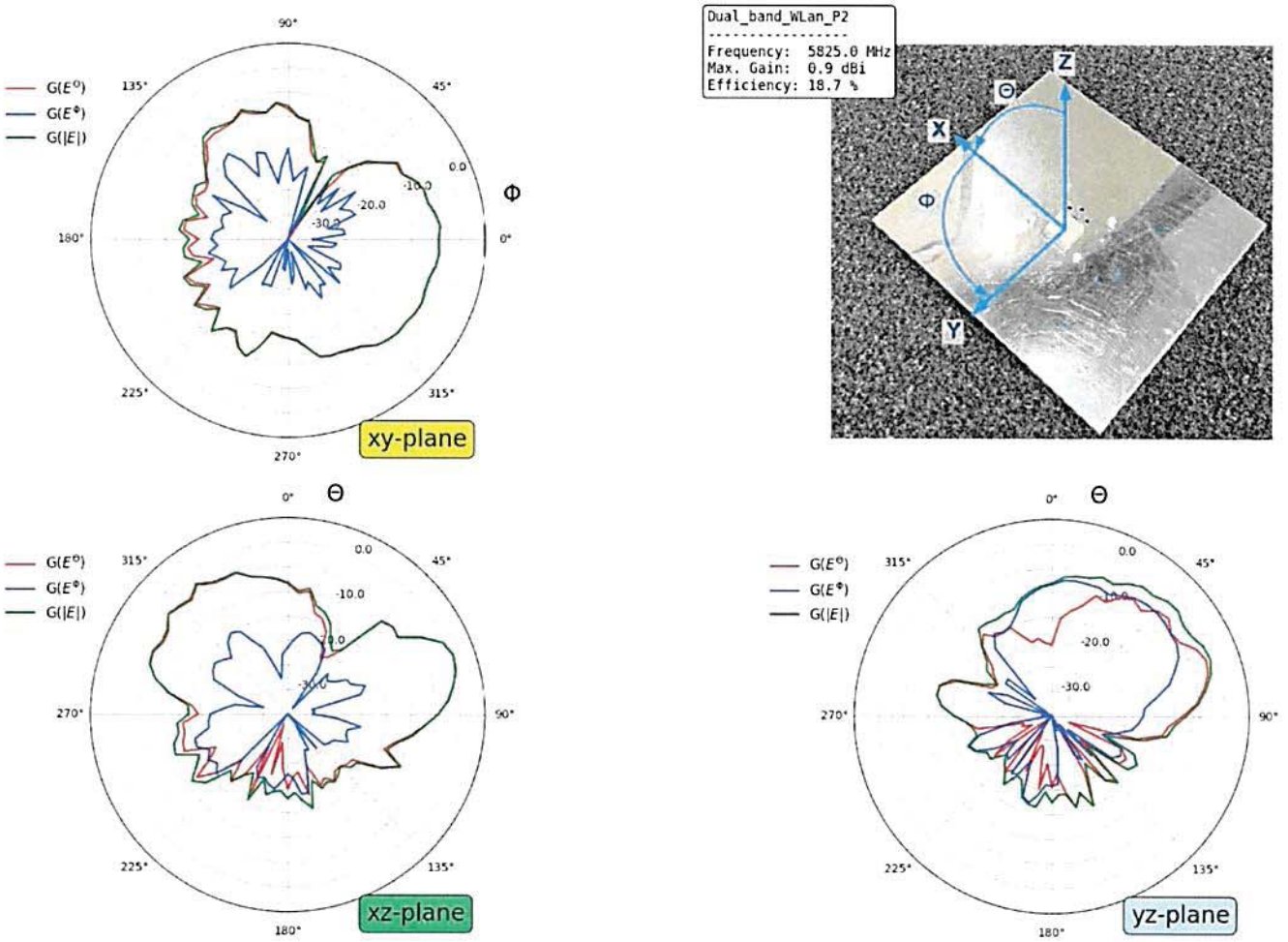

Figure 9-16: E-Theta/E-Phi/Sum polar diagram, port2 @ 5825 MHz